NeuroImage: Clinical 11 (2016) 539–547

Contents lists available at ScienceDirect

NeuroImage: Clinical

journal homepage: www.elsevier.com/locate/ynicl

Choosing the polarity of the phase-encoding direction in diffusion MRI: Does it matter for group analysis?

M. Kennis[a,b,*], S.J.H. van Rooij[a,b,c], R.S. Kahn[a], E. Geuze[a,b], A. Leemans[d]

[a]Brain Center Rudolf Magnus, Department of Psychiatry, University Medical Center Utrecht, Utrecht, The Netherlands
[b]Research Center, Military Mental Healthcare, Ministry of Defence, Utrecht, The Netherlands
[c]Department of Psychiatry and Behavioral Sciences, Emory University School of Medicine, Atlanta, GA, USA
[d]Image Sciences Institute, University Medical Center Utrecht, Utrecht, The Netherlands

ARTICLE INFO

Article history:
Received 2 December 2015
Received in revised form 10 March 2016
Accepted 31 March 2016
Available online 12 April 2016

Keywords:
Phase-encoding polarity
Diffusion tensor imaging
Fractional anisotropy
EPI distortions
Susceptibility artifacts
Data quality
Group analysis

ABSTRACT

Notorious for degrading diffusion MRI data quality are so-called susceptibility-induced off-resonance fields, which cause non-linear geometric image deformations. While acquiring additional data to correct for these distortions alleviates the adverse effects of this artifact drastically – e.g., by reversing the polarity of the phase-encoding (PE) direction – this strategy is often not an option due to scan time constraints. Especially in a clinical context, where patient comfort and safety are of paramount importance, acquisition specifications are preferred that minimize scan time, typically resulting in data obtained with only one PE direction. In this work, we investigated whether choosing a different polarity of the PE direction would affect the outcome of a specific clinical research study. To address this methodological question, fractional anisotropy (FA) estimates of *FreeSurfer* brain regions were obtained in civilian and combat controls, remitted posttraumatic stress disorder (PTSD) patients, and persistent PTSD patients before and after trauma-focused therapy and were compared between diffusion MRI data sets acquired with different polarities of the PE direction (posterior-to-anterior, PA and anterior-to-posterior, AP). Our results demonstrate that regional FA estimates differ on average in the order of 5% between AP and PA PE data. In addition, when comparing FA estimates between different subject groups for specific cingulum subdivisions, the conclusions for AP and PA PE data were not in agreement. These findings increase our understanding of how one of the most pronounced data artifacts in diffusion MRI can impact group analyses and should encourage users to be more cautious when interpreting and reporting study outcomes derived from data acquired along a single PE direction.

1. Introduction

Diffusion tensor imaging (DTI) is a popular approach for studying white matter microstructural characteristics (Basser et al., 1994; Jones and Leemans, 2011; Pierpaoli et al., 1996) and has been applied in a wide range of clinical applications (Menon, 2011; O'Hanlon et al., 2015; Reijmer et al., 2015; Verhoeven et al., 2012; Wang et al., 2012). To minimize scan times, diffusion MRI data are generally acquired with echo-planar imaging (EPI) (Turner and Le Bihan, 1990). A major disadvantage of acquiring DTI data with EPI, however, is the presence of susceptibility-induced geometric distortions (Andersson et al., 2003; Gallichan et al., 2010; Jezzard and Balaban, 1995; Jones and Cercignani, 2010; Ruthotto et al., 2012). These distortions are generally visible as geometric image deformations in combination with signal expansion (signal loss) or compression (signal pile up) in the phase-encoding (PE) direction and have been shown to affect global fractional anisotropy (FA) values (Wu et al., 2008) and tractography results (Irfanoglu et al., 2012).

As susceptibility-induced distortions can be more harmful in data acquired along the left-to-right PE orientation (blurring signals across the midline and hampering the natural symmetry of the left and right brain hemispheres) than in data with anterior-to-posterior (AP) or posterior-to-anterior (PA) PE directions, the latter is most frequently applied in diffusion MRI of the brain (Glover et al., 2012). To correct for EPI distortions, diffusion images can be normalized to an anatomical scan without EPI distortions (e.g., to a T_1 or T_2 weighted image as described in Irfanoglu et al., 2012). Although more advanced methods to correct for distortions are currently available, these come at the cost of requiring additional information (e.g., two sets of diffusion images, acquired with opposite PE, or a B0-field map characterizing the magnetic field inhomogeneity (Irfanoglu et al., 2015)). Especially in a clinical context, where scan times are kept minimal, it is therefore common practice to obtain only one set of diffusion images with one specific PE direction in anterior-to-posterior (AP) or posterior-to-anterior (PA)

* Corresponding author at: University Medical Center Utrecht, Psychiatry / MGGZ OC, Heidelberglaan 100, Huispostnummer A01.1.43, 3584 CX Utrecht, The Netherlands.
E-mail address: mitzykennis@gmail.com (M. Kennis).

http://dx.doi.org/10.1016/j.nicl.2016.03.022

direction and, subsequently, to apply a registration-based procedure for correcting EPI distortions. However, whether FA estimates derived with a typical analysis pipeline differ significantly between scans with a different PE direction remains unclear. Investigating this potential confound is particularly relevant for clinical research applications, where such type of image artifact could affect conclusions.

In this study we investigate the magnitude and significance of the effect of PE direction on FA estimates in specific brain regions by comparing DTI data sets with opposing PE direction. In addition to exploring regional FA differences between the PA and AP PE DTI data, we investigated whether the outcome of a specific clinical research question would be in agreement between PA and AP PE scans. In particular, for this study, we questioned whether the observed FA changes in specific cingulum subdivisions – brains areas known to be affected in PTSD (e.g., Abe et al., 2006; Daniels et al., 2013; Fani et al., 2012; Kim et al., 2007; Zhang et al., 2011) – differs between (a) PTSD patients who recovered after treatment (remitted PTSD); (b) veterans who still had a PTSD diagnosis after treatment (persistent PTSD); and (c) combat controls. Similar outcomes for the clinical research question were expected for parallel processed AP and PA PE scans.

2. Material and methods

2.1. Participants and clinical assessment

PTSD patients were recruited from one of the four outpatient clinics of the Military Mental Healthcare Organization, after a clinician diagnosed PTSD. Healthy civilian and combat controls were recruited with advertisements. After written and verbal explanation of the study was given, all participants gave informed consent. In total, 352 sets of DTI scans (i.e., 176 scans with PA PE direction and 176 scans with AP PE direction) were obtained to investigate the effect of the polarity of the PE on the FA estimates. Of those, 171 scans were paired with a T1 weighted image, which allowed registration based correction, and investigation of *FreeSurfer* parcellations. This included scans from 25 healthy civilian controls, 28 healthy veterans and 51 PTSD patients at the first time point, and scans at reassessment of 22 healthy veterans and 45 PTSD patients.

All veterans (with and without PTSD) were reassessed after 6–8 months, during which PTSD patients received treatment as usual (see Supplementary material A for an overview of the clinical assessment, the inclusion and exclusion criteria, and details of the demographics of the participants). Based on PTSD diagnosis at reassessment, PTSD patients were subdivided into a remitted group (no PTSD diagnosis at reassessment, $N = 16$), and a persistent PTSD group (PTSD diagnosis at reassessment, $N = 23$). This study was approved by the medical ethical committee of the University Medical Center Utrecht and was performed in accordance with the Declaration of Helsinki (World Medical Association, 2013).

2.2. Data acquisition

Two transverse DTI data sets with opposite polarity of the PE direction (i.e., PA and AP) were acquired, each consisting of one non-diffusion weighted image ($b = 0$ s/mm^2) and 30 diffusion-weighted images ($b = 1000$ s/mm^2) (Jones, 2004). Other acquisition settings were: TR = 7057 ms, TE = 68 ms, matrix size = 128 × 128, voxel size = 1.875 × 1.875 × 2 mm^3, no gap, echo train length = 35, SENSE factor = 3, FOV = 240 × 240 mm^2, 75 slices, slice thickness = 2 mm, scan time = 4:21 min. The acquisition details for the T1-weighted high-resolution scan, obtained during the same scan session, were TR = 10 ms, TE = 4.6 ms, flip angle = 8°, 200 sagittal slices, FOV = 240 × 240 mm^2, matrix size = 304 × 299, voxel size = 0.8 × 0.8 × 0.8 mm^3.

2.3. Data processing

ExploreDTI (v4.8.4) (Leemans et al., 2009) was used to process each DTI dataset, which consisted of correcting for subject motion, eddy current-induced distortions, and susceptibility artifacts (Irfanoglu et al., 2012; Leemans and Jones, 2009). Of note, this correction procedure does not include a modulation with the Jacobian determinant of the deformation field. The diffusion tensor was estimated on the corrected images with a robust fitting routine (Tax et al., 2015; Veraart et al., 2013).

In order to investigate difference in FA estimates before registration-based correction, native space white matter skeletons were created using FSL (Smith et al., 2006; with default setting: FA threshold > 0.2). Mean FA-values were extracted and compared between PA and AP PE acquisition. To investigate the effect of PE direction on FA-values, mean FA values were extracted from parallel processed (corrected) AP and PA images for 70 cortical white matter regions and 27 subcortical regions as derived with *FreeSurfer* (Fischl et al., 2002; Fischl, 2012) (see Fig. 1).

2.3.1. Illustration of correction for susceptibility artifacts

Fig. 2 presents an overview of the procedure to correct for susceptibility-induced artifacts. The top row shows the color-encoded FA maps after correcting for subject motion and eddy current-induced distortions, but *before* the susceptibility correction step (left: PA PE direction; right: AP PE direction). On these maps – and their enlarged regions in the middle – one can easily appreciate the differences in geometry of the brain stem area between the AP and PA scans. Also frontal brain areas are heavily affected as can be seen on the non-diffusion-weighted images (middle row). By registering the dMRI data to the T1 weighted data with *ExploreDTI*, whereby the deformation field is constrained to the PE direction (for details, see Irfanoglu et al., 2012), one can correct the susceptibility-induced artifacts (bottom row). The bottom left and bottom right images show the color-encoded FA maps *after* the susceptibility correction step and fused with the T1 weighted image. These corrected images were used for regional FA comparison between PA an AP PE acquisition.

While correcting for EPI deformations improves the quality of the data geometry, residual misalignment between the T1 weighted and corrected diffusion-weighted data can still often be observed. Fig. 3 shows an example where such spatial correspondence is not optimal. Especially in the frontal area, where these artifacts are quite pronounced, the difference in geometry between AP and PA PE data is clearly visible (see enlarged regions in Fig. 3). In short, AP and PA PE datasets were processed in parallel with *ExploreDTI* and the corrected images were utilized to calculate FA values and assess the difference in regional FA-values between AP and PA PE acquisition.

2.4. Statistical analyses

2.4.1. Native space white matter skeleton FA difference

A paired samples *t*-test was performed to investigate the difference between native space white matter skeleton mean FA values for PA and AP PE scans ($N = 176$). Note that this analysis was performed before the registration-based correction step.

2.4.2. Regional FA differences

The absolute difference and the percentage difference in FA values between PA and AP PE directions was calculated for each *FreeSurfer* region over all available registration-based corrected FA maps. For each region, a paired samples *t*-test was performed using the FA values of the PA and AP PE scans for all groups and time points combined ($N = 171$). Bonferroni correction was applied ($p < 0.05/97 = 0.0005$ was deemed significant) to correct for testing multiple brain areas. The absolute and percentage FA differences were also displayed on the "FS_cvs_avg35_inMNI152" *FreeSurfer* template (Fischl, 2012).

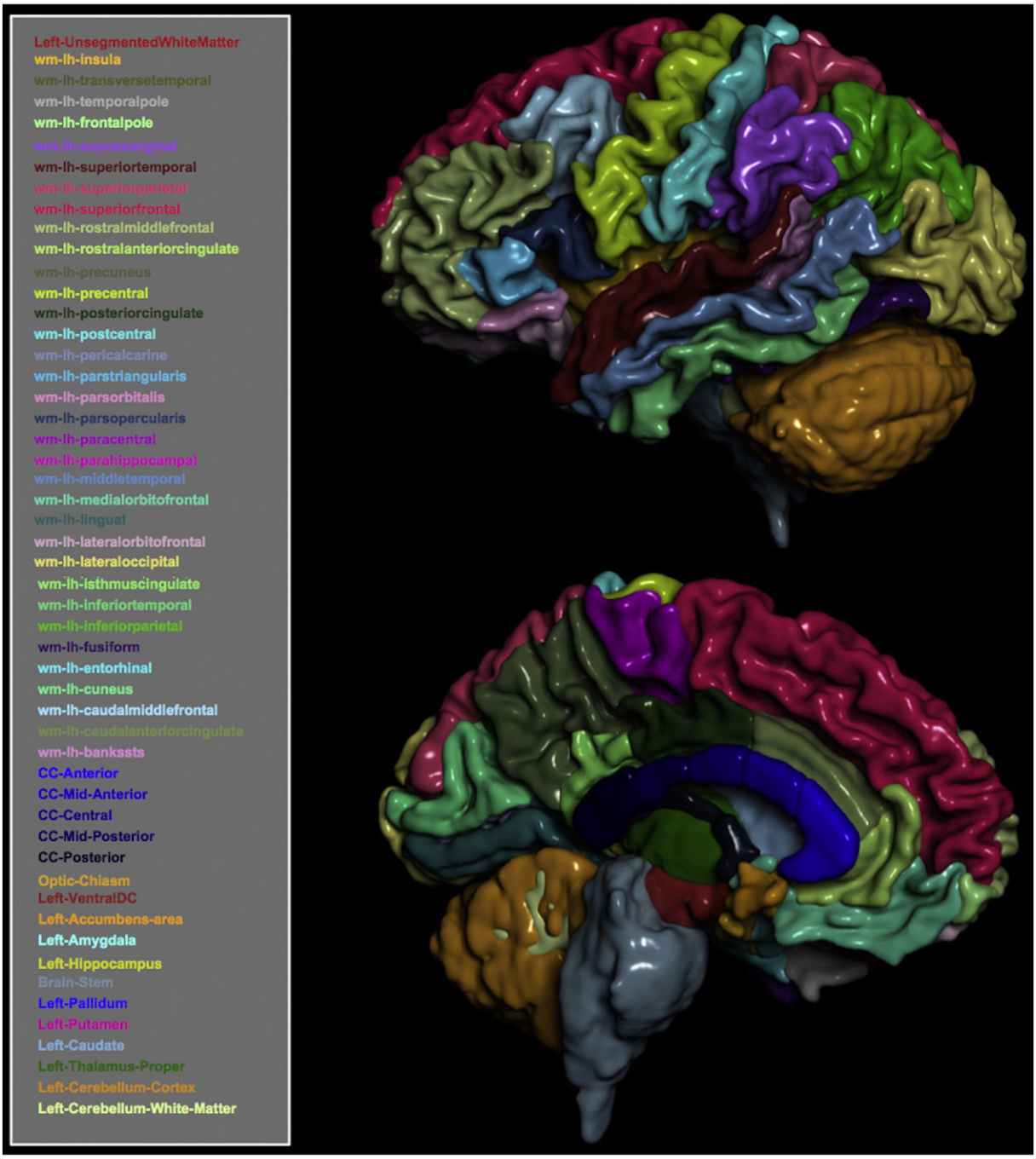

Fig. 1. Surface rendering of *FreeSurfer* parcellations for the left hemisphere of a representative subject. A list of *FreeSurfer* white matter and subcortical brain regions included in the analyses is shown on the left with color-coding corresponding to the surface rendering.

2.4.3. Clinical research question

To answer the clinical research question, i.e., whether the observed FA changes in specific cingulum subdivisions were different between (a) remitted PTSD (b) persistent PTSD and (c) combat controls over the course of treatment, repeated measures ANOVAs (group (3) by time (2) by hemisphere (2)) were performed to compare the rostral, caudal, posterior, isthmus and hippocampal cingulum subdivisions, for the two sets of reversed PE diffusion images, using age as covariate. Since we were not interested in asymmetry of the cingulum, hemisphere was modeled as a parameter of non-interest to provide overall statistics for the left and right cingulum subdivisions combined. To correct for testing five subdivisions of the cingulum, Bonferroni correction was applied ($p < 0.05/5 = 0.01$ was deemed significant), as well as false discovery rate (FDR) correction.

3. Results

3.1. Native space white matter skeleton FA difference

Comparison of the white matter skeleton FA estimates revealed that FA for PA (FA $= 0.441 \pm 0.012$) was higher than FA for AP (FA $= 0.434 \pm 0.010$). Interestingly, this difference, while being small, is highly significant (paired-sample t-test; $N = 176$ per group; $p < 0.0001$).

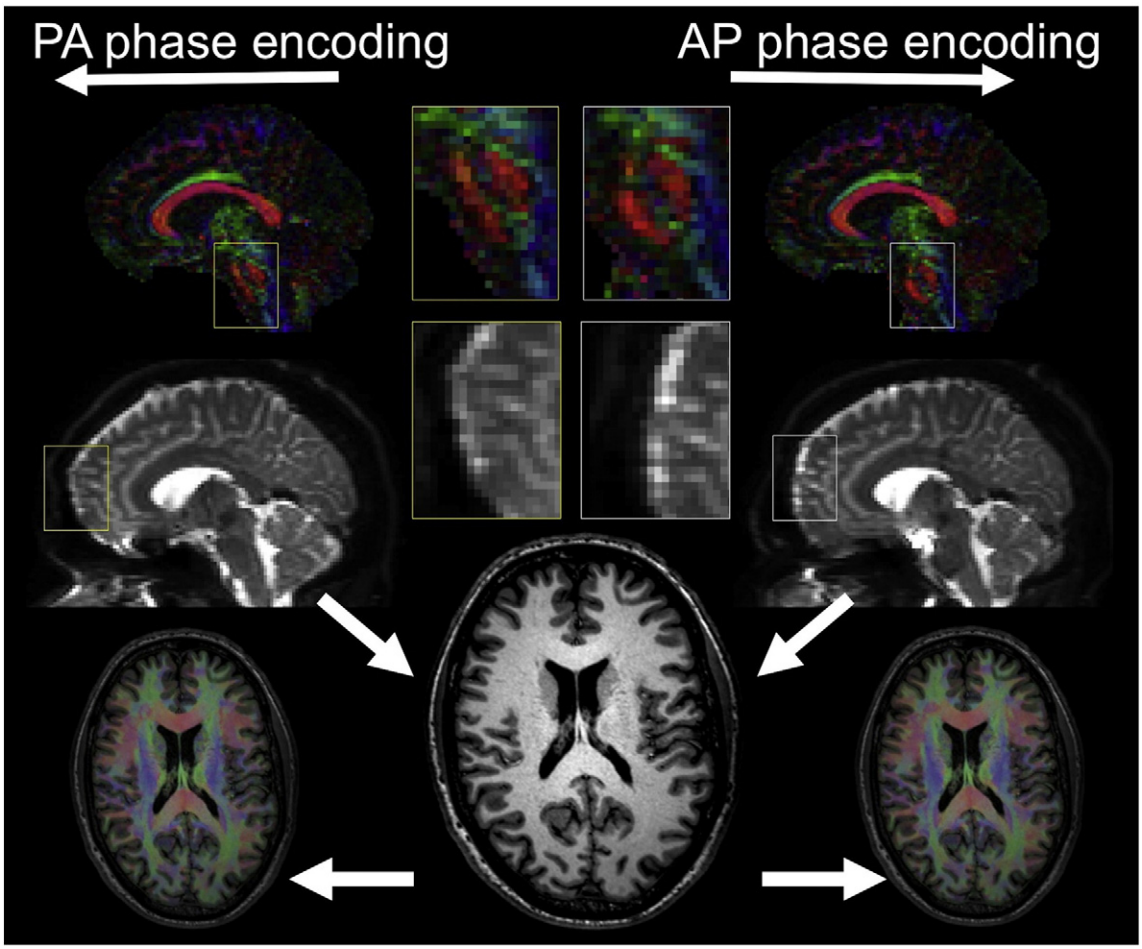

Fig. 2. Susceptibility-induced artifacts and their differences due to polarity of PE direction (PA: left vs. AP: right). Top and middle rows show the color-encoded fractional anisotropy and non-diffusion-weighted images, respectively, which were already corrected for subject motion and eddy current distortions. Notice the difference in geometry between the AP and PA PE scans as shown in the enlargements. The bottom row shows the color-encoded diffusion orientation fused with the T1 weighted image, which was used for correcting the susceptibility-induced artifacts.

Fig. 4 illustrates that PA FA estimates were higher than AP estimates for nearly all diffusion scan pairs.

3.2. Regional FA differences

The spatial distribution of FA estimates of *FreeSurfer* brain regions of PA and AP PE scans (corrected for subject motion, eddy currents and susceptibility distortions) for all subjects at both time points ($N = 171$) showed similar patterns, but differences in FA were also visible, for example in the posterior corpus callosum and inferior parietal white matter (Fig. 5). The FA magnitude difference between PA and AP PE direction scans ($N = 171$ for each PE direction) ranged from 0.001 to 0.06 or, equivalently, from 0.4% to 30% across all *FreeSurfer* regions, and was on average 0.014 or 4.5% (Fig. 6). The FA values were significantly different between PA and AP scans for many of the *FreeSurfer* regions (for a complete list see Supplementary material B). Regions that showed the largest positive "PA minus AP" differences in FA (i.e., with differences > 0.03) were the optic chiasm (0.06 or 30%), left inferior parietal (0.04 or 12%), left lateral occipital (0.03 or 12%), and left bankSSTS (0.03 or 9%). Regions with the largest negative "PA minus AP" differences in FA (i.e., with differences < −0.03) were the middle posterior corpus callosum (−0.04 or −7%), posterior corpus callosum (−0.04 or −6%), right temporal pole (−0.03, −11%), right pars orbitalis (−0.03 or −11%), and right frontal pole (−0.03 or −15%).

From Fig. 6 one can observe that the largest FA differences between the PA and PA PE direction scans were located in regions closest to the interface between brain and non-brain tissue. In addition, positive FA differences (PA > AP) were located more frequently in the left hemisphere than in the right hemisphere (Fig. 6).

3.3. Clinical research question

The DTI scans with AP PE direction showed a main effect of group for the FA of the isthmus cingulum ($F_{(2,56)} = 5.318$, $p = 0.008$, Bonferroni and FDR corrected), where remitted PTSD patients had significantly lower FA values than persistent PTSD patients and controls (Fig. 7). The scans with PA PE direction showed a similar pattern, i.e., a main effect of group for the FA of the isthmus cingulum ($F_{(2,56)} = 4.490$, $p = 0.016$), but this effect did not survive Bonferroni, nor FDR correction (Fig. 7). No interaction effects were observed for the FA of the isthmus cingulum. No group or group-by-time interaction effects were found for either PA or AP PE data for the FA of the other cingulum white matter subdivisions.

4. Discussion

Susceptibility-induced artifacts are known to hamper diffusion scan quality, though it was unclear to what extent the polarity of PE direction matters for FA estimates, especially for group analyses. Here, a large set of diffusion images with opposing polarity of PE direction (AP or PA) was utilized to examine effects of the choice of PE direction on FA estimates, and on the outcome of a specific clinical research

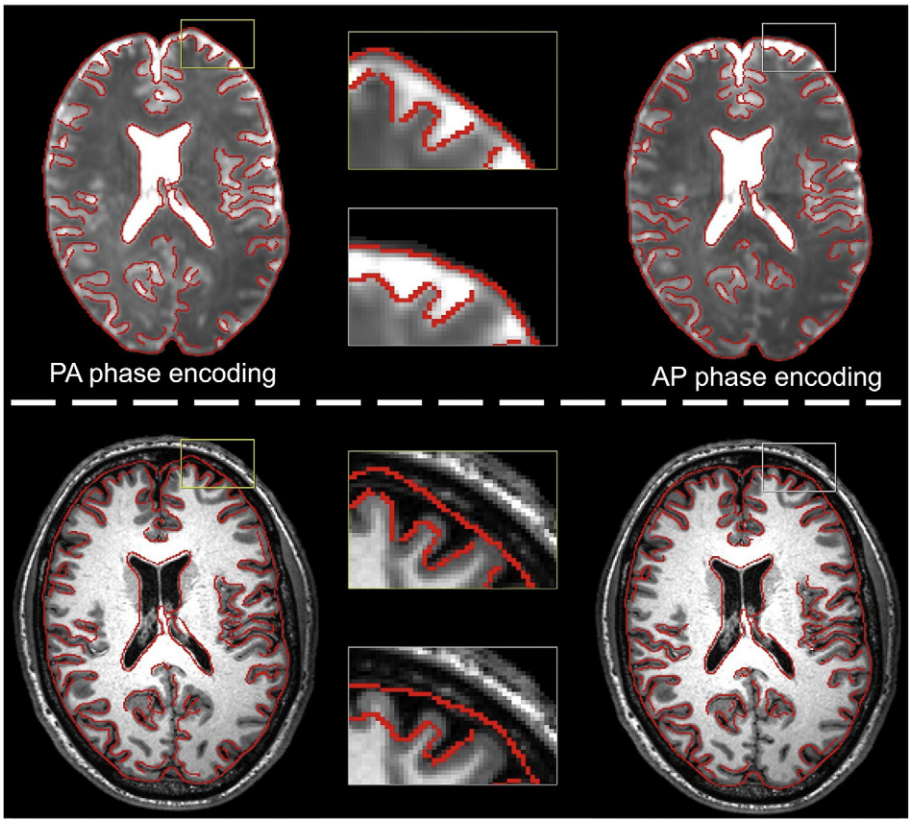

Fig. 3. Illustration of the difference in residual spatial misalignment between AP and PA PE data after distortion correction. Edges (grey/white matter boundary) of the non-diffusion-weighted image (top) are displayed in red and overlaid on the T1 weighted image (bottom) for both PA (left) AP (right) PE for a representative subject.

question. While several methods have been proposed to correct for susceptibility-induced artifacts, e.g., by mapping the (static or dynamic) B0 magnetic field inhomogeneity (Chen et al., 2006; Jezzard and Balaban, 1995; Truong et al., 2011), by applying advanced reconstruction approaches (Bhushan et al., 2013), or by collecting additional diffusion scans (Andersson et al., 2003; Andersson and Sotiropoulos, 2015; Gallichan et al., 2010; Irfanoglu et al., 2015; Morgan et al., 2004; Ruthotto et al., 2012), many of these strategies are not feasible in a clinical setting as they require specific sequences or hardware specs that are not widely available yet or come at the price of additional scan time. In this study, we focused on comparing AP and PA PE scans by using a registration-based distortion correction procedure. To this end, the T1-weighted scan served as the undistorted target as it is typically available in conventional clinical MRI acquisition protocols. Native space white matter skeleton FA values were also investigated in order to provide insights in FA differences before the registration-based correction.

4.1. White matter skeleton and regional FA differences

Differences in FA values between parallel processed PA and AP PE scans were observed for 85 of the 97 investigated *FreeSurfer* brain regions, and were on average in the order of 5%. The magnitude of this effect is similar to the magnitude of differences in FA estimates between clinical groups (e.g., Phan et al., 2009; Tromp et al., 2012). Moreover, in 26 *FreeSurfer* brain regions, the effect of the choice in PE direction was even larger than 5%, suggesting that the effect of interest (e.g., the group effect) could potentially be swamped by the effect of PE direction in those brain regions.

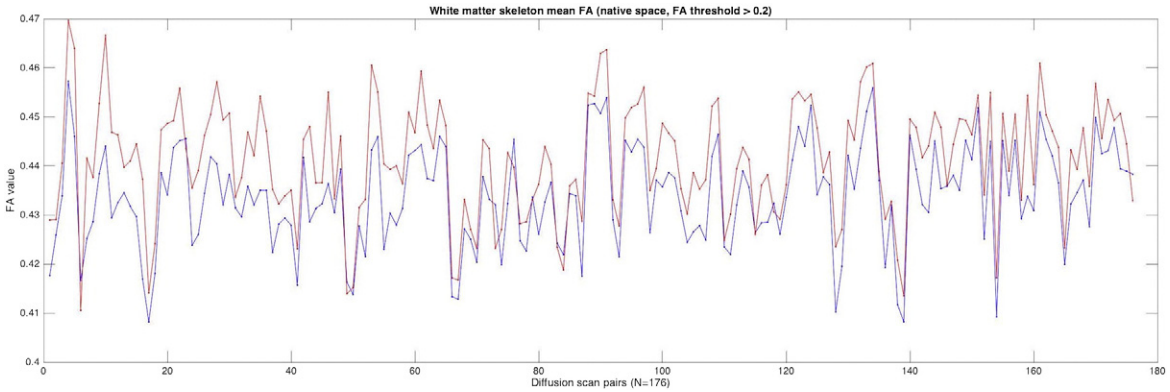

Fig. 4. Mean FA values for native space white matter skeletons (FA threshold > 0.2) for PA and AP PE direction ($N = 176$ diffusion scan pairs).

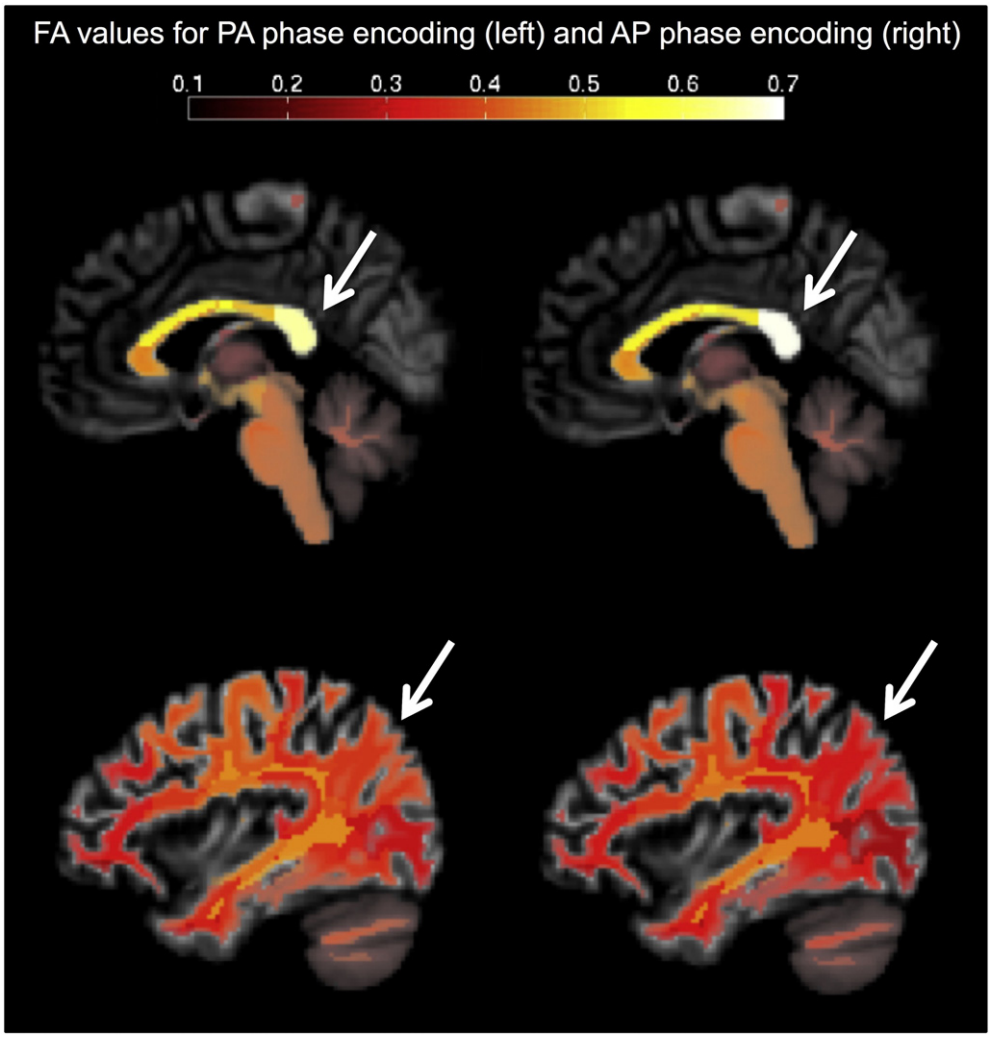

Fig. 5. Posterior corpus callosum and inferior parietal white matter FA estimates of PA and AP PE scans over all participants ($N = 171$ for each PE direction).

There are mainly two factors that can be the driving the observed difference in FA values between the PA and AP PE scans. First, the local differences in signal intensity between the PA and AP PE scans (signal pile-up vs. signal loss) cause a local difference in signal-to-noise ratio, which, in turn, may result in differences in the estimation bias. Secondly, the FA differences between the PA and AP PE scans could also be attributed to methodological imperfections of the correction procedure, in which residual misalignment between the corrected diffusion scans and the anatomical T1-weighted scan can still be present (Fig. 3). However, the native space white matter skeleton FA estimates also differed significantly between PA and AP PE direction (Fig. 4). Since these skeletons were based on native space images, no misalignment is involved and, hence, the difference observed in white matter skeleton FA value is likely due to the estimation bias induced by susceptibility distortions. Therefore, it can also be suggested that the regional FA differences are not solitarily due to misalignment, but probably also suffer from estimation bias.

Another observation was that the difference in FA estimates between opposing PE direction scans was not the same across regions. In some regions, scans with PA PE direction provided higher FA estimates than scans with AP PE direction (see positive difference, i.e., the "red-ish" brain areas in Fig. 6), whereas the opposite was found in other brain regions (see negative difference, i.e., the "blue-ish" brain areas in Fig. 6). Furthermore, higher FA values in PA versus AP PE scans seemed to be more frequently present in the left hemisphere with lower FA values in PA versus AP PE being more frequently observed in the right hemisphere. Consequently, one could argue that the choice in polarity of the PE direction could even affect lateralization outcomes of diffusion measures. Potentially, natural asymmetries in white matter connectivity and tract volume (Büchel et al., 2004; de Groot et al., 2009; Thiebaut de Schotten et al., 2011) may explain the hemispheric differences, since misalignment will have a larger impact on smaller structures than on larger structures. Note that this observation was only qualitative of nature, as investigating asymmetry was considered beyond the scope of this study. In addition, the coloring (blue for negative red for positive) shows quite a visually striking distinction between the left and right hemisphere, although there is practically no difference in absolute FA values (in the order of $|0.01|$ on average). Future research would be needed to investigate the interaction between the effect of PE direction (and the strategy to correct for it), natural asymmetries in white matter connectivity, and lateralization measures to further elucidate this observation.

4.2. Clinical research question

The effect of the choice of the polarity of PE direction (AP or PA) on the outcome of the clinical research question, i.e., whether the observed FA changes in specific cingulum subdivisions were different between (a) remitted PTSD (b) persistent PTSD and (c) combat controls over the course of treatment, was clearly not negligible. While both PA and AP PE diffusion scans showed an uncorrected group difference in FA for the isthmus cingulum, only for the AP PE data this group effect

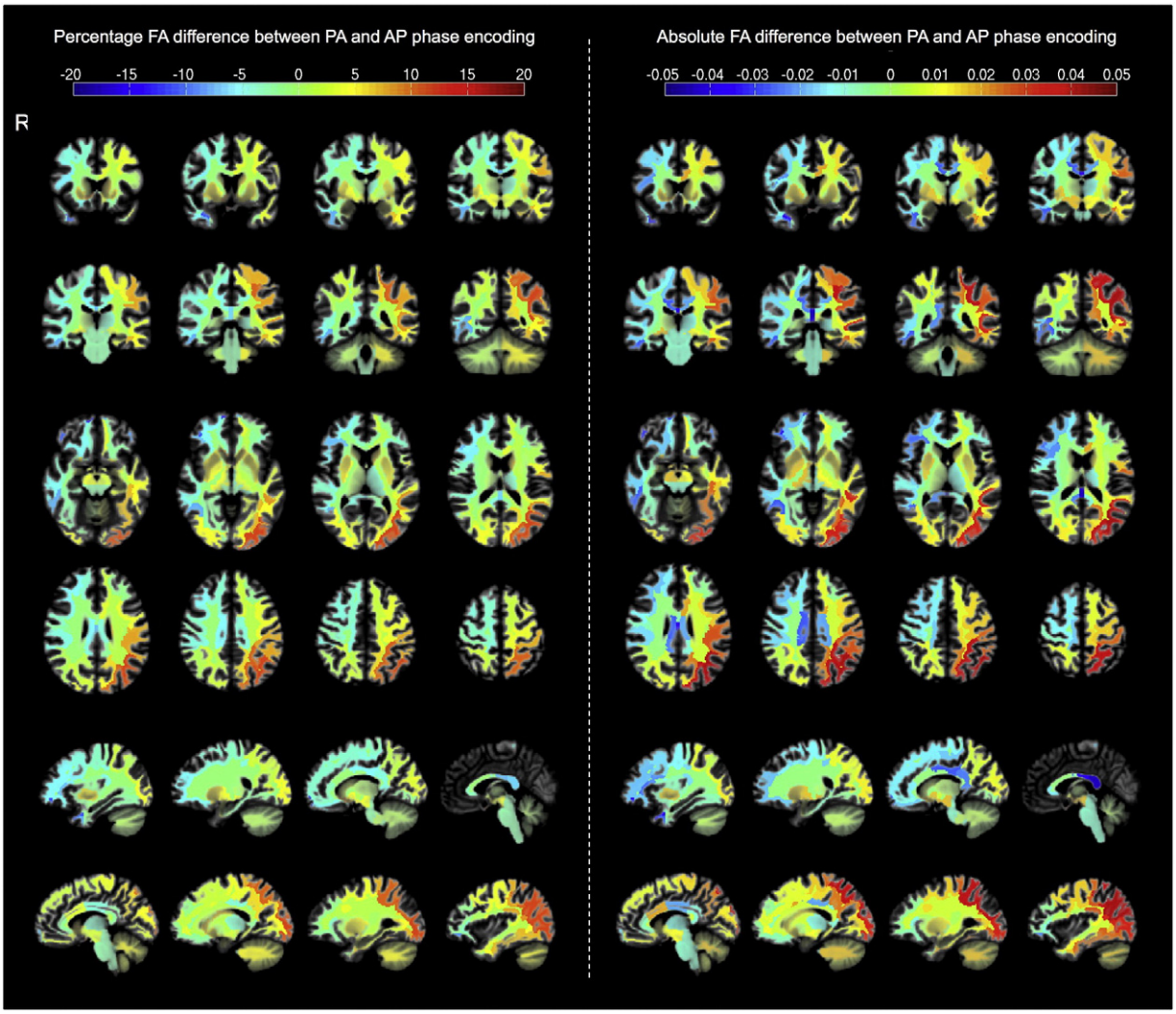

Fig. 6. Percentage and absolute FA difference between PA and AP PE over all participants ($N = 171$ for each PE direction).

survived the Bonferroni correction for multiple comparisons. Therefore, the conclusions drawn from both group analyses for the data acquired with different polarity of PE direction in this study are not in agreement. As a general guideline, we encourage researchers to also report the polarity of the PE direction to be able to compare their findings more objectively between future studies.

4.3. Methodological considerations

The two sets of DTI scans were acquired in the same order: the PA PE before the AP PE direction. Therefore, multiple slow scanner drifts may have affected the quality of the scans, and possibly have interacted with the PE effect (Truong et al., 2011; Vos et al., 2014). In addition, the differences in FA estimates were compared between scans with opposing polarity of PE, and not between different distortion correction methods (e.g., compare registration-based methods with reversed PE polarity methods such as Top-up of FSL (Andersson et al., 2003; Andersson and Sotiropoulos, 2015)). While such comparison could also provide valuable insights, we have specifically chosen for this analysis strategy as it reflects the typical pipeline for group studies in a clinical setting, which was the main goal of this study. In addition, it is inevitable that the processing pipelines would differ between reversed PE correction methods and registration-based correction, which would complicate interpretation. Future studies should investigate the difference in FA values between registration-based approaches (as applied here) and reversed PE based corrections. More specifically, it would be interesting to see if reversed PE correction will provide intermediate FA values with respect to PA and AP parallel processed estimates.

As an alternative to the time consuming distortion corrections that require collecting reversed PE acquisition of all diffusion images, it can be proposed to acquire reversed PE B0 images only to calculate the displacement field (Andersson and Sotiropoulos, 2015), which can then be utilized for correction. This will only add a minimal amount of time to the scan protocol (e.g., 7s in this study). Future studies should explore the quality of such a distortion correction in comparison with acquiring all diffusion images with reversed PE and with registration-based approaches. In addition, accuracy of FA estimates was investigated in this study, which does not provide information about the precision of the estimates. Future research can also investigate differences in precision of FA estimates between AP and PA PE acquisition, using perturbation analyses, such as bootstrapping or error propagation methods, which can be useful for calculating uncertainty measures (Chang et al., 2007; Koay et al., 2007; Pajevic and Basser, 2003; Whitcher et al., 2008).

Finally, the number of subjects in the remitted ($N = 16$) group could be considered relatively small for investigating the clinical research question. However, with such confounding effects not commonly evaluated with data from large samples of subjects, nor in clinical populations (Irfanoglu et al., 2015; Wu et al., 2008), our study complements currently available methodological studies by providing investigation

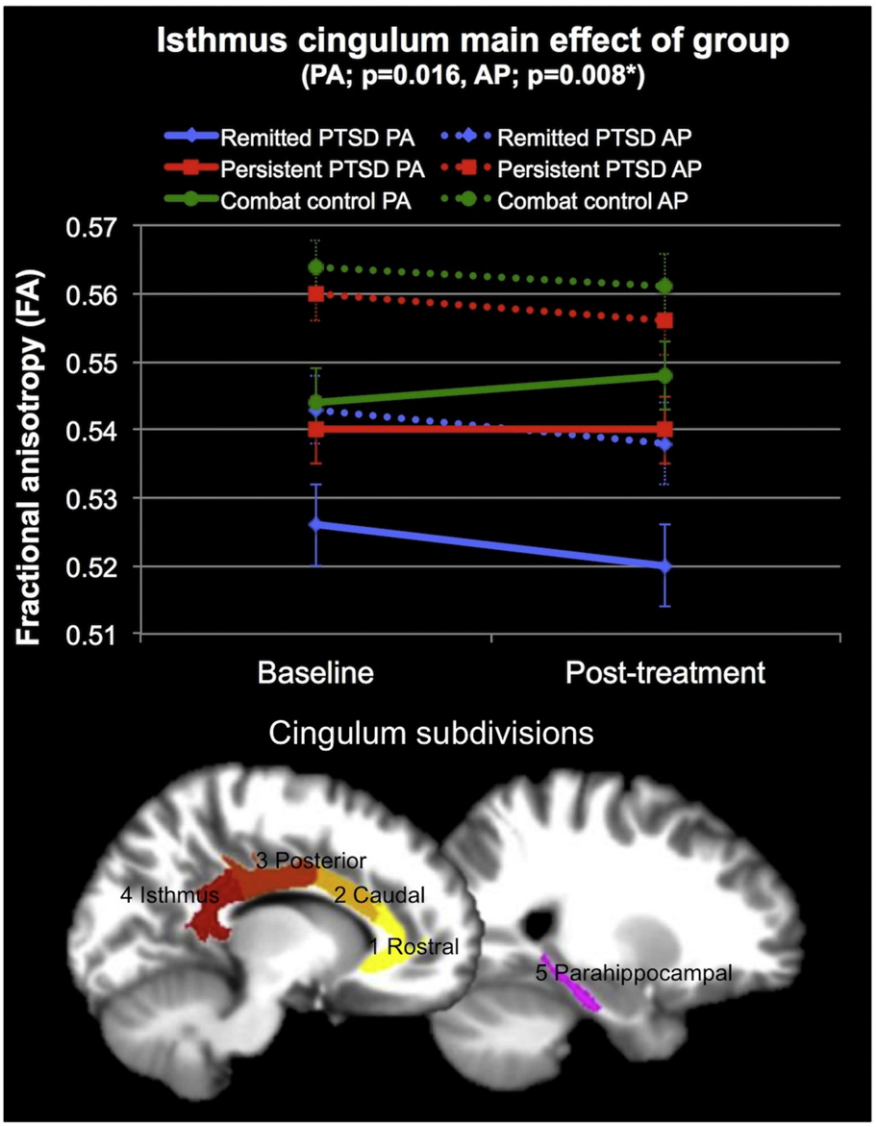

Fig. 7. Main effect of group for the isthmus cingulum subdivision for PA and AP PE (top). The investigated subdivisions of the cingulum are also presented (bottom).

of the effect of PE direction in a large sample of scans, and between groups.

5. Conclusion

In this study, choosing a different polarity of the PE direction (AP versus PA) was shown to affect the estimation of FA values in 85 of the 97 investigated *FreeSurfer* brain regions. In addition, we have shown that the conclusions for the clinical research question outcome of the AP and PA PE data did not concur. While our study highlights the importance of choice of the polarity of the PE direction in a DTI group analysis using registration-based correction, other diffusion models will suffer from this confound in a similar fashion. These findings increase our understanding of how one of the most pronounced data artifacts in diffusion MRI can impact group studies and should encourage users to be more cautious when interpreting and reporting study outcomes derived from data acquired along a single PE direction.

Acknowledgements

This research was financially supported by the Dutch Ministry of Defence. The research of A.L. is supported by VIDI Grant 639.072.411 from the Netherlands Organization for Scientific Research (NWO). We thank Rachel Sjouwerman for her help with the *FreeSurfer* segmentation.

Appendix A. Supplementary data

Supplementary data to this article can be found online at http://dx.doi.org/10.1016/j.nicl.2016.03.022.

References

Abe, O., Yamasue, H., Kasai, K., Yamada, H., Aoki, S., Iwanami, A., Ohtani, T., Masutani, Y., Kato, N., Ohtomo, K., 2006. Voxel-based diffusion tensor analysis reveals aberrant anterior cingulum integrity in posttraumatic stress disorder due to terrorism. Psychiatry Res. Neuroimaging 146 (3), 231–242.

Andersson, J.L.R., Sotiropoulos, S.N., 2015. An integrated approach to correction for off-resonance effects and subject movement in diffusion MR imaging. NeuroImage http://dx.doi.org/10.1016/j.neuroimage.2015.10.019.

Andersson, J.L.R., Skare, S., Ashburner, J., 2003. How to correct susceptibility distortions in spin-echo echo-planar images: application to diffusion tensor imaging. NeuroImage 20 (2), 870–888.

Basser, P.J., Mattiello, J., LeBihan, D., 1994. MR diffusion tensor spectroscopy and imaging. Biophys. J. 66 (1), 259–267.

Bhushan, C., Joshi, A.A., Leahy, R.M., Haldar, J.P., 2013. Improved B0-distortion correction in diffusion MRI using interlaced q-space sampling and constrained reconstruction. Magn. Reson. Med. 72 (5), 1218–1232.

Büchel, C., Raedler, T., Sommer, M., Sach, M., Weiller, C., Koch, M.A., 2004. White matter asymmetry in the human brain: a diffusion tensor MRI study. Cereb. Cortex 14 (9), 945–951.
Chang, L.C., Koay, C.G., Pierpaoli, C., Basser, P.J., 2007. Variance of estimated DTI-derived parameters via first-order perturbation methods. Magn. Reson. Med. 57 (1), 141–149.
Chen, B., Guo, H., Song, A.W., 2006. Correction for direction-dependent distortions in diffusion tensor imaging using matched magnetic field maps. NeuroImage 30 (1), 121–129.
Daniels, J.K., Lamke, J., Gaebler, M., Walter, H., Scheel, M., 2013. White matter integrity and its relationship to PTSD and childhood trauma — a systematic review and meta-analysis. Depress. Anxiety 30 (3), 207–216.
de Groot, M., Vernooij, M., Klein, S., Leemans, A., de Boer, R., van der Lugt, A., Breteler, M., Niessen, W., 2009. Asymmetry analysis along the entire cingulum in the general population. NeuroImage 47 (Supplement 1), S105.
Fani, N., King, T.Z., Jovanovic, T., Glover, E.M., Bradley, B., Choi, K., Ely, T., Gutman, D.A., Ressler, K.J., 2012. White matter integrity in highly traumatized adults with and without post-traumatic stress disorder. Neuropsychopharmacology 37 (12), 2740–2746.
Fischl, B., 2012. FreeSurfer. NeuroImage 62 (2), 774–781.
Fischl, B., Salat, D.H., Busa, E., Albert, M., Dieterich, M., Haselgrove, C., Van Der Kouwe, A., Killiany, R., Kennedy, D., Klaveness, S., et al., 2002. Whole brain segmentation: automated labeling of neuroanatomical structures in the human brain. Neuron 33 (3), 341–355.
Gallichan, D., Andersson, J.L.R., Jenkinson, M., Robson, M.D., Miller, K.L., 2010. Reducing distortions in diffusion-weighted echo planar imaging with a dual-echo blip-reversed sequence. Magn. Reson. Med. 64 (2), 382–390.
Glover, G.H., Mueller, B.A., Turner, J.A., Van Erp, T.G.M., Liu, T.T., Greve, D.N., Voyvodic, J.T., Rasmussen, J., Brown, G.G., Keator, D.B., et al., 2012. Function biomedical informatics research network recommendations for prospective multicenter functional MRI studies. J. Magn. Reson. Imaging 36 (1), 39–54.
Irfanoglu, M.O., Walker, L., Sarlls, J., Marenco, S., Pierpaoli, C., 2012. Effects of image distortions originating from susceptibility variations and concomitant fields on diffusion MRI tractography results. NeuroImage 61 (1), 275–288.
Irfanoglu, M.O., Modi, P., Nayak, A., Hutchinson, E.B., Sarlls, J., Pierpaoli, C., 2015. DR-BUDDI (diffeomorphic registration for blip-up blip-down diffusion imaging) method for correcting echo planar imaging distortions. NeuroImage 106 (0), 284–299.
Jezzard, P., Balaban, R.S., 1995. Correction for geometric distortion in echo planar images from B(o) field variations. Magn. Reson. Med. 34 (1), 65–73.
Jones, D.K., 2004. The effect of gradient sampling schemes on measures derived from diffusion tensor MRI: a Monte Carlo study. Magn. Reson. Med. 51 (4), 807–815.
Jones, D.K., Cercignani, M., 2010. Twenty-five pitfalls in the analysis of diffusion MRI data. NMR Biomed. 23 (7), 803–820.
Jones, D.K., Leemans, A., 2011. Diffusion tensor imaging. Methods Mol. Biol. 711, 127–144.
Kim, S.J., Jeong, D.-, Sim, M.E., Bae, S.C., Chung, A., Kim, M.J., Chang, K.H., Ryu, J., Renshaw, P.F., Lyoo, I.K., 2007. Asymmetrically altered integrity of cingulum bundle in posttraumatic stress disorder. Neuropsychobiology 54 (2), 120–125.
Koay, C.G., Chang, L.-C., Pierpaoli, C., Basser, P.J., 2007. Error propagation framework for diffusion tensor imaging via diffusion tensor representations. IEEE Trans. Med. Imaging 26 (8), 1017–1034.
Leemans, A., Jones, D.K., 2009. The B-matrix must be rotated when correcting for subject motion in DTI data. Magn. Reson. Med. 61 (6), 1336–1349.
Leemans, A., Jeurissen, B., Sijbers, J., Jones, D., 2009. ExploreDTI: a graphical toolbox for processing, analyzing, and visualizing diffusion MRI data. Proceedings of the 17th Annual Meeting of International Society for Magnetic Resonance in Medicine, p. 3537.
Menon, V., 2011. Large-scale brain networks and psychopathology: a unifying triple network model. Trends Cogn. Sci. 15 (10), 483–506.
Morgan, P.S., Bowtell, R.W., McIntyre, D.J.O., Worthington, B.S., 2004. Correction of spatial distortion in EPI due to inhomogeneous static magnetic fields using the reversed gradient method. J. Magn. Reson. Imaging 19 (4), 499–507.
O'Hanlon, E., Leemans, A., Kelleher, I., Clarke, M.C., Roddy, S., Coughlan, H., Harley, M., Amico, F., Hoscheit, M.J., Tiedt, L., et al., 2015. White matter differences among adolescents reporting psychotic experiences: a population-based diffusion magnetic resonance imaging study. JAMA Psychiatry 72 (7), 668–677.
Pajevic, S., Basser, P.J., 2003. Parametric and non-parametric statistical analysis of DT-MRI data. J. Magn. Reson. 161 (1), 1–14.
Phan, K.L., Orlichenko, A., Boyd, E., Angstadt, M., Coccaro, E.F., Liberzon, I., Arfanakis, K., 2009. Preliminary evidence of white matter abnormality in the uncinate fasciculus in generalized social anxiety disorder. Biol. Psychiatry 66 (7), 691–694.
Pierpaoli, C., Jezzard, P., Basser, P.J., Barnett, A., Di Chiro, G., 1996. Diffusion tensor MR imaging of the human brain. Radiology 201 (3), 637–648.
Reijmer, Y.D., Fotiadis, P., Martinez-Ramirez, S., Salat, D.H., Schultz, A., Shoamanesh, A., Ayres, A.M., Vashkevich, A., Rosas, D., Schwab, K., et al., 2015. Structural network alterations and neurological dysfunction in cerebral amyloid angiopathy. Brain J. Neurol. 138 (Pt 1), 179–188.
Ruthotto, L., Kugel, H., Olesch, J., Fischer, B., Modersitzki, J., Burger, M., Wolters, C.H., 2012. Diffeomorphic susceptibility artifact correction of diffusion-weighted magnetic resonance images. Phys. Med. Biol. 57 (18), 5715–5731.
Smith, S.M., Jenkinson, M., Johansen-Berg, H., Rueckert, D., Nichols, T.E., Mackay, C.E., Watkins, K.E., Ciccarelli, O., Cader, M.Z., Matthews, P.M., Behrens, T.E., 2006. Tract-based spatial statistics: voxelwise analysis of multi-subject diffusion data. NeuroImage 31 (4), 1487–1505.
Tax, C.M., Otte, W.M., Viergever, M.A., Dijkhuizen, R.M., Leemans, A., 2015. REKINDLE: robust extraction of kurtosis INDices with linear estimation. Magn. Reson. Med. 73 (2), 794–808.
Thiebaut de Schotten, M., Ffytche, D.H., Bizzi, A., Dell'Acqu, F., Alli, M., Walshe, M., Murray, R., Williams, S.C., Murphy, D.G.M., Catani, M., 2011. Atlasing location, asymmetry and inter-subject variability of white matter tracts in the human brain with MR diffusion tractography. NeuroImage 54 (1), 49–59.
Tromp, D.P.M., Grupe, D.W., Oathes, D.J., McFarlin, D.R., Hernandez, P.J., Kral, T.R.A., Lee, J.E., Adams, M., Alexander, A.L., Nitschke, J.B., 2012. Reduced structural connectivity of a major frontolimbic pathway in generalized anxiety disorder. Arch. Gen. Psychiatry 69 (9), 925–934.
Truong, T., Chen, N., Song, A.W., 2011. Dynamic correction of artifacts due to susceptibility effects and time-varying eddy currents in diffusion tensor imaging. NeuroImage 57 (4), 1343–1347.
Turner, R., Le Bihan, D., 1990. Single-shot diffusion imaging at 2.0 tesla. J. Magn. Reson. (1969) 86 (3), 445–452.
Veraart, J., Sijbers, J., Sunaert, S., Leemans, A., Jeurissen, B., 2013. Weighted linear least squares estimation of diffusion MRI parameters: strengths, limitations, and pitfalls. NeuroImage 81, 335–346.
Verhoeven, J.S., Rommel, N., Prodi, E., Leemans, A., Zink, I., Vandewalle, E., Noens, I., Wagemans, J., Steyaert, J., Boets, B., et al., 2012. Is there a common neuroanatomical substrate of language deficit between autism spectrum disorder and specific language impairment? Cereb. Cortex 22 (10), 2263–2271.
Vos, S.B., Tax, C.M.W., Visser, F., Luijten, P.R., Leemans, A., Froeling, M., 2014. Importance of correcting for B0-drift-induced global signal decrease in diffusion MRI. Int. Soc. Magn. Reson. Med. 4460.
Wang, H.C., Hsu, J.L., Leemans, A., 2012. Diffusion tensor imaging of vascular Parkinsonism: structural changes in cerebral white matter and the association with clinical severity. Arch. Neurol. 69 (10), 1340–1348.
Whitcher, B., Tuch, D.S., Wisco, J.J., Sorensen, A.G., Wang, L., 2008. Using the wild bootstrap to quantify uncertainty in diffusion tensor imaging. Hum. Brain Mapp. 29 (3), 346–362.
World Medical Association, 2013. Declaration of Helsinki: ethical principles for medical research involving human subjects. JAMA - J. Am. Med. Assoc. 310 (20), 2191–2194.
Wu, M., Chang, L.C., Walker, L., Lemaitre, H., Barnett, A.S., Marenco, S., Pierpaoli, C., 2008. Comparison of EPI distortion correction methods in diffusion tensor MRI using a novel framework. Med. Image Comput. Comput. Assisted Interv. 11 (Pt 2), 321–329.
Zhang, L., Zhang, Y., Li, L., Li, Z., Li, W., Ma, N., Hou, C., Zhang, Z., Zhang, Z., Wang, L., et al., 2011. Different white matter abnormalities between the first-episode, treatment-naive patients with posttraumatic stress disorder and generalized anxiety disorder without comorbid conditions. J. Affect. Disord. 133 (1–2), 294–299.